International Journal of Medical, Medicine and Health Sciences
ISSN: 2517-9969
Vol:3, No:6, 2009

Multilayer Soft Tissue Continuum Model: Towards Realistic Simulation of Facial Expressions

A. Hung, K. Mithraratne, M. Sagar, and P. Hunter

***Abstract*—**A biophysically based multilayer continuum model of the facial soft tissue composite has been developed for simulating wrinkle formation. The deformed state of the soft tissue block was determined by solving large deformation mechanics equations using the Galerkin finite element method. The proposed soft tissue model is composed of four layers with distinct mechanical properties. These include stratum corneum, epidermal-dermal layer (living epidermis and dermis), subcutaneous tissue and the underlying muscle. All the layers were treated as non-linear, isotropic Mooney Rivlin materials. Contraction of muscle fibres was approximated using a steady-state relationship between the fibre extension ratio, intracellular calcium concentration and active stress in the fibre direction. Several variations of the model parameters (stiffness and thickness of epidermal-dermal layer, thickness of subcutaneous tissue layer) have been considered.

***Keywords*—**Bio-physically based, soft tissue mechanics, facial tissue composite, wrinkling.

I. Introduction

FACIAL expression simulation has always been a key research area in the animation industry. Even with the assistance of sophisticated animation software, tremendous human effort is still required to create realistic facial expressions. Early simulations of the face used geometric techniques that require low computational cost. However, this can no longer fulfil the increasing user expectations and has led to the development of physically and anatomically based modelling techniques to produce more realistic results. Accurate simulation of the human face is not only important to the animation industry but also assists cranio-facial surgery planning and the facial reconstruction process in forensic investigations.

A. Skin

Skin forms the outermost layer of the body including the face. Like any soft tissue, the mechanical properties of skin are dependent on its structure and constituents. Skin is composed of two major layers: the epidermis (0.06mm – 0.1mm thick) and the dermis (2-4mm thick). The epidermis can be further subdivided into five layers and the most superficial layer is known as the stratum corneum. Stratum corneum is relatively thin and has a very strong tensile strength as the dense coating of dead cells on the surface is rich in insoluble keratin proteins, while the rest of the epidermis is composed of softer living cells. The stiffness of stratum corneum is estimated to be 1000 times than skin [1]. The second layer of skin, the dermis, is made up of a network of strong collagen fibres (up to 30% by volume) and elastin fibres embedded in a matrix of ground substances. The interwoven collagen fibres provide strength while the rubber-like elastin fibres account for the skin's elastic behaviour [2].

Skin is made up of various fibrous, vascular and amorphous components that make it a non-homogeneous and visco-elastic material. The stress-strain relation of skin is non-linear and the typical tensile force versus strain curve is shown in Fig. 1.

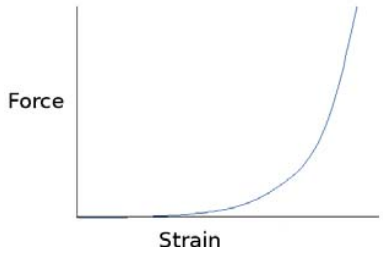

Fig. 1 Tensile force versus strain curve for skin

The shape of this curve is primarily characterised by the physical transformation of cutaneous fibres. At low tension levels, fibres, which were initially undulated and randomly oriented, gradually straighten and align with the load axis. During this phase of stretching, the skin modulus is low. Once the fibres are aligned in the same direction, the tensile strength of the tissues increases significantly and this is reflected in the steep slope of the curve [3]. The transformation of cutaneous fibres under tension load have been detailed in many microscopic studies including Brown's [4], but their roles in the mechanical response of skin under compression remain unclear.

The soft tissues present beneath the skin are collectively known as the subcutaneous tissues. They are mainly loose connective tissues responsible for sustaining the integrity of body structures. It is common to find fat deposits directly underneath the dermis (known as hypodermis) [2], but subcutaneous fatty tissues can be missing in certain anatomical regions e.g. under the eye lids [5].

A. Hung, K. Mithraratne and P. Hunter are with Auckland Bioengineering Institute, University of Auckland, Private Bag 92019, Auckland, New Zealand
M. Sagar is with WETA Digital Ltd., P. O. Box. 15208, Wellington, New Zealand.

B. Facial Muscles

The contraction of specific muscles on the face produces a facial expression. and facial muscles are innervated by the seventh cranial nerve which is known as the facial nerve [5]. When nerve impulses reach a muscle, it causes a release of neurotransmitter at the neuromuscular junction (where the nerve endings meet the muscle) and evokes a potential change in the muscle cell membrane. This is followed by an increase of intracellular free calcium ions that initiate the contraction process [6]. The model presented in this paper uses the steady state fibre activation model proposed by Hunter [7] to activate the contraction of muscles.

C. Existing Facial Models

One of the earliest facial modelling techniques was key-framing. It required exact topologies to be known at more than one time points and intermediate frames were created using interpolation functions [8]. Further development was done by Parke [9], who extended this technique by introducing parameterised models. This allowed the animator to create a wider variation of facial shapes and expressions by manipulating facial parameters like degree of jaw rotation, jaw width and nose length. These are geometrically based techniques that are fast for real time simulations but the computed deformation does not cohere to any principle of physics or biomechanics and also ignores the underlying anatomy.

Keeve et al. [10], on the other hand, modelled the skin and muscle layers using deformable spring lattices. The assigned element spring stiffness was based on the elasticity of the soft tissue layer, the layer thickness and the size of the tissue elements. Koch et al. [11] refined this approach by the addition of another spring connection with the neighbouring nodes on the underlying layer and had numerically determined the spring stiffness constants using Visible Human Data images. Recent models are aiming for more anatomical accuracies. Sifakis et al. [12] constructed a model based on digitised facial musculature using Magnetic Resonance Imaging (MRI) data of a living subject. They used an activation-based force function to simulate muscle contractions and developed an algorithm that automatically determines the muscle activations using motion capturing data. Facial models have also been developed for medical purposes. Chabanas [13] was able to predict the surgical results from bone repositioning using a multilayer (dermis, hypodermis, muscle) finite element soft tissue model. The mechanical properties of the tissue layers were specified using Young's modulus and Poisson ratio with the assumption of linear elastic behaviour.

D. Models of Wrinkle Simulation

Zhang and Sim [14] simulated wrinkle formation using a linear muscle model coupled with a wrinkle amplitude function. Li and Yin [15] proposed an geometrically based algorithm for producing wrinkle movements on wrinkle regions of the face. Wu et al. [16][17] used B-spline patches to represent muscles in their layered facial model. The contraction of muscles propagates the tension to the skin membrane layer through spring connections. Wrinkles were simulated by defining the nodal wrinkle magnitude as a function of strain of the local skin nodes. Instead of taking the geometric approach, Flynn [18] predicted skin deformation under uniaxial compression using a continuum model and wrinkles were successfully simulated by modelling skin as an inhomogeneous material where a different constitutive law is used for each skin layer (stratum corneum, dermis, hypodermis). The importance of representing skin as an inhomogeneous material in wrinkle simulation has also been emphasised by Magnenat-Thalmann et al [19].

The aim of the present study is to develop a biophysically based continuum model of facial soft tissue composite with a view of simulating wrinkle formation due to the contraction of underlying muscles in the face. In the next section, the details of the finite element model for large deformation mechanics together with constitutive models for tissue layers and the fibre activation model are discussed. Simulations results on wrinkle formation in response to muscle activation are presented in the following section. Finally, the effect of simulation parameters on wrinkle formation is detailed.

II. Methods

A. Finite Element Model

The deformation of the multilayer soft tissue continuum was obtained by solving the static Cauchy equation,

$$\frac{\partial \sigma_{ij}}{\partial x_j} + \rho b_f = 0 \,. \tag{1}$$

where σ_{ij} are Cauchy stress tensor components, x_j are the spatial coordinates, ρ is the tissue density and b_f are the body force components. The above governing equation was solved using the Galerkin finite element (FE) method with suitable displacement boundary conditions together with the fibre activation model described in section C below. The non-linear algebraic equations generated from the weak from of the governing equation based on the Galerkin FE method were solved using the Newton-Raphson iterative method.

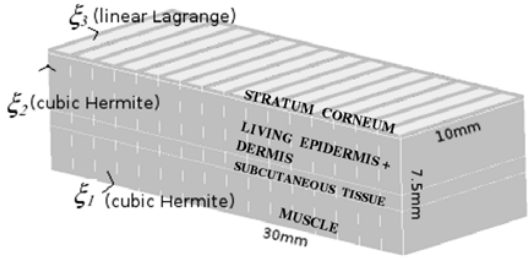

Fig. 2 Facial Composite Model

The facial composite is logically separated into four layers due to the significant differences in mechanical properties between the layers: stratum corneum, living epidermis + dermis, subcutaneous tissue and muscle (Fig. 2). The soft living epidermis is thin (around 2.5% of the dermal thickness) and is considered to be insignificant thus the living epidermis

and dermis are represented as a single layer (epidermal-dermal layer) in this model.

This finite element model uses high order elements as opposed to the linear approach in previous studies. The tissue composite consists of 64 bicubic Hermite-linear Lagrange elements resulting in a total of 2040 nodal degrees of freedom (DOFs).

The nodal DOFs were interpolated using cubic Hermite interpolation functions for the element directions 1 and 2 (ξ_1 and ξ_2) while a linear Lagrange interpolation function was used for the third element direction, ξ_3. With this interpolation scheme, both C^0 and C^1 continuity is maintained in ξ_1 and ξ_2 directions. The wrinkling occurs mainly in the ξ_1 direction as the muscle fibres, which generate contractile force, follow ξ_1 direction. Since ξ_3 direction is parallel to the width of the tissue block and due to its symmetry in that direction, higher order interpolation in ξ_3 direction is not required.

B. Constitutive Equations

All the layers of the FE model are considered as non-linear isotropic Mooney Rivlin materials where the strain energy density function (SEDF), w is given as:

$$w=c_{10}(I_1-3)+c_{01}(I_2-3)+c_{11}(I_1-3)(I_2-3)+c_{20}(I_1-3)^2+\ldots+p(I_3-1) \quad (2)$$

where c_{10},c_{01},.. are experimentally determined material constants, I_1,I_2 and I_3 are principal invariants (scalar) of the right Cauchy deformation tensor and p is the hydrostatic pressure due to incompressibility.

The use of scalar invariants assumes the described material to be isotropic. The last term of the SEDF function is the energy contribution from hydrostatic pressure, this is equivalent to zero for incompressible materials and all layers are assumed to be incompressible in the proposed model. Values of the Mooney-Rivlin material constants for the facial tissue composite layers chosen for simulations are given in Table I.

TABLE I
MOONEY-RIVLIN CONSTANTS FOR FACIAL COMPOSITE

Layer	**Mooney Rivlin constants in kPa (all other constants are set to zero)**	**Source**
Stratum Corneum	C_{10} = 9400 C_{11}= 82000	Approximated based on Leveque's estimation [1] on the relative stiffness of stratum corneum
Living Epidermis + Dermis	C_{10} = 9.4 C_{11}= 82	[20]
Subcutaneous Tissue	C_{10} = 3	Approximated.
Muscle	C_{10} = 10 C_{20}= 10 C_{30}= 6.67	Typical material constants for skeletal muscle [21]

C. Fibre Activation Model

The force generated by muscle fibres upon stimulation is initiated by the release of Ca^{2+}. Although the process of the Calcium binding to Troponin-C and ensuing activation of myofibres is time dependent, the steady state model proposed by Hunter [7] was used in this study. According to this model, the relationship between the active fibre stress (force) and Ca^{2+} concentration is given by

$$\sigma_a=\frac{\left[Ca^{2+}.\left(Ca^{2+}\right)_{\max}\right]^h}{\left[Ca^{2+}.\left(Ca^{2+}\right)_{\max}\right]^h+\left[\left(Ca^{2+}\right)_{50}\right]^h}.\sigma_{a,ref}.\left[1+\beta.(\lambda-1)\right] \quad (3)$$

where Ca^{2+} is the calcium concentration corresponding to current activation level, $(Ca^{2+})_{max}$ is the maximum intracellular calcium concentration and $(Ca^{2+})_{50}$ is the value corresponding to 50% of the maximum tension. h is the Hill coefficient and β and λ are the slope parameter and fibre extension ratio respectively. $\sigma_{a,ref}$ represents the value at $\lambda = 1.0$.

Once the active stress component (σ_a) in the fibre direction is determined using equation (3), it is then converted to the corresponding second Piola-Kirchhoff (2PK) stress components and added to the passive stress component of the 2PK stress tensor ($T_{passive}$). Hence the total 2PK stress tensor (T_{total}) given as:

$$\mathbf{T}_{\mathbf{total}} = \mathbf{T}_{\mathbf{passive}} + J\mathbf{F}^{-1}\boldsymbol{\sigma}_{\mathbf{ff}}\mathbf{F}^{-\mathbf{T}} \quad (4)$$

where

$$\mathbf{T}_{\mathbf{passive}} = \frac{\partial w}{\partial \mathbf{E}} \qquad \sigma_{\mathbf{ff}} = \begin{bmatrix} \sigma_a & 0 & 0 \\ 0 & 0 & 0 \\ 0 & 0 & 0 \end{bmatrix}$$

F = deformation gradient tensor
J = Jacobian of **F**
E = Green Lagrange strain tensor

Table II below gives the values of various parameters used in equation (3).

TABLE II
PARAMETERS FOR FIBRE ACTIVATION MODEL

Parameter	**Value**
$\sigma_{a,ref}$	100.0 kPa
β	1.45
$(Ca^{2+})_{50}$	0.5 nM
$(Ca^{2+})_{max}$	1.0 nM
h	3.0

III. SIMULATION RESULTS

The FE computational model described above was implemented using the software package CMISS [22], developed at the Bioengineering Institute. CMISS is a mathematical modelling environment that allows the application of finite element analysis, boundary element and collocation techniques to a variety of complex bioengineering problems.

Measurements were taken from one of the Visible Human Data images [23] to approximate the thickness of each layer. The region measured was where the Frontalis muscle located (Fig. 3).

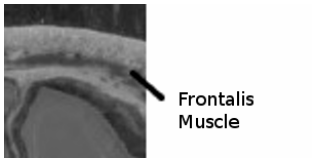

Fig. 3 Extract of a Visible Human image [23] (transverse view from top) showing the left frontal region

The thickness is assumed to be uniform within each layer and is approximated as followed: stratum corneum: 0.02 mm, living epidermis + dermis: 3.96 mm, subcutaneous tissue: 0.96mm, muscle: 2.56 mm. The dimensions of the tissue block were set to 30 mm long (estimated length of the Frontalis muscle), 11mm wide and 7.5 mm deep and as was mentioned, composed of 64 bicubic Hermite - linear Lagrange elements (Fig. 2).

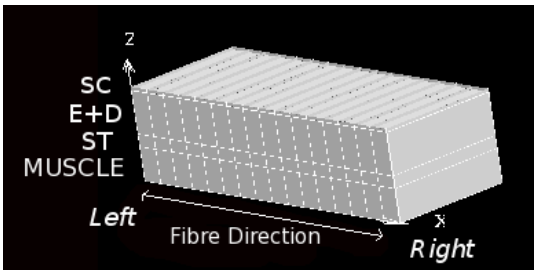

Fig. 4 Undeformed state of the facial composite model (SC = stratum corneum, E + D = living epidermis + dermis, ST = subcutaneous tissue)

The nodes on the left wall (Fig. 4) were geometrically fixed and the bottom nodes were constrained to move only within the bottom plane (boundary conditions). The muscle contraction along the fibre direction was controlled by changing the calcium concentration level of the activation model. The sliding effect between the subcutaneous layer and muscle due to the presence of fascia has been ignored and the layers are connected by tightly coupled nodes. The final deformed state is shown in Fig. 5. This was determined by solving for the equilibrium state at a calcium concentration of 0.9. The amplitude and wavelength of the wrinkle formed are 1.16 mm and 9.14 mm respectively.

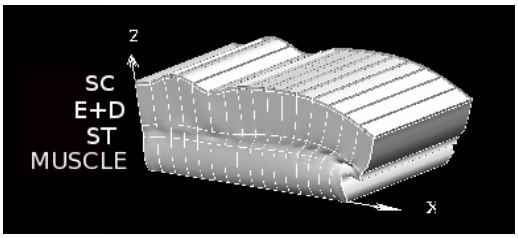

Fig. 5 Deformed state of the facial composite model (SC = stratum corneum, E + D = living epidermis + dermis, ST = subcutaneous tissue)

The following scenarios were investigated with a calcium concentration of 0.6 and the resulting deformed states of the facial composite are shown in Fig. 7 - 10:

1. Stratum corneum layer is assigned with the same material parameters as the epidermal-dermal layer - Skin is modelled as a homogeneous material. (Fig. 7)
2. c_{10} and c_{11} of the epidermal-dermal layer are halved - The collagen density decreases as age increases [24]. It is assumed collagen fibre is the dominant mechanical component for resisting compressive load in the dermis. (Fig. 8)
3. Thickness of the subcutaneous tissue layer is doubled – representing the richness in fat in the subcutaneous layer of the cheek. (Fig. 9)
4. The thickness of the epidermal-dermal layer is halved – some regions of the body, e.g. the volar forearm, has thinner skin. (Fig. 10)

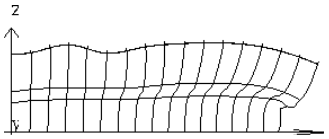

Fig. 6 Deformed state of the original model

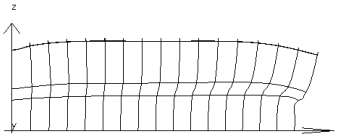

Fig. 7 Deformed state of scenario 1 (modelled skin as a homogeneous material)

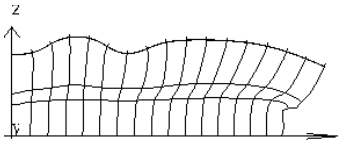

Fig. 8 Deformed state of scenario 2 (reduced stiffness in epidermal-dermal layer)

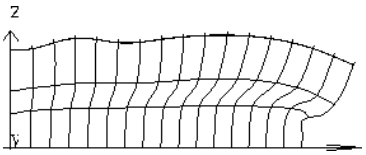

Fig. 9 Deformed state of scenario 3 (Thicker subcutaneous tissues)

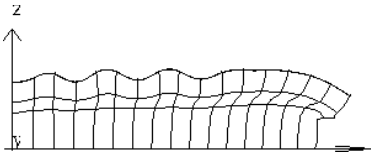

Fig. 10 Deformed state of scenario 4 (Thinner epidermal-dermal layer)

IV. Conclusion

The model developed to simulate wrinkling in facial soft tissue composite in this study considered large deformation mechanics, non-linear constitutive properties and active contraction of muscle fibres. The Galerkin finite element method was used to obtain the deformed state (wrinkled) of the composite. The rationale for using high order cubic Hermite elements is to provide a computationally efficient model of muscle structure (especially fibre orientation) in relation to the geometry of the model. Preserving derivative continuity of the fibre directions and describing fibre directions in relation to anatomical shape is very important for anatomical accuracy and computational efficiency.

The inability of the model to simulate wrinkles shown in Fig. 7 emphasised the importance of considering the inhomogeneity of skin. Several variations of the model parameters have been considered and the predicted results correlate reasonably well with the typical observations of expressive wrinkles: (i) mature skin, which contains relatively less collagen, is not as stiff and a deeper fold is formed under the same activation (Fig. 8) (ii) wrinkle is less likely to form in regions where the subcutaneous tissue layer is thick. (Fig. 9) (iii) wrinkle density is higher on thinner skin (Fig. 10).

V. Discussions

The proposed model can be improved by representing the skin or the subcutaneous tissues using the Lanir constitutive model [25]. The Lanir model defines the mechanical properties based on the contribution and the degree of undulation of each fibre type present in the tissue. It is capable of characterising the viscous and anisotropic effects that are neglected in the Mooney Rivlin model.

Further investigations are needed for choosing an appropriate discretisation scheme for this finite element model. Reducing element dimensions can potentially lead to a more spatially converged solution that comes with a cost of increased computational time. An attempt has been made to increase the level of discretisation in direction of ξ_1 and ξ_2. The additional degrees of freedoms have increased the numerical instability of the model and the computational process failed to complete for a sufficient level of activation. The future approach is to treat the relatively thin stratum corneum layer as a 2D membrane (application of membrane mechanics) and solve the problem as a coupled membrane-solid system. Also, realistic geometry of anatomical structures like muscles and skull will be incorporated into this model in the future.

Acknowledgement

The work presented in this paper was funded by the Foundation for Research, Science and Technology (FoRST) of New Zealand under the research contract number UOAX0712.

References

[1] Leveque, J. L. "Influence of ageing on the in vivo extensibility of human skin at a low stress" Archives of Dermatological Research, 1980, 269, pp. 127.
[2] Wood, E. J. and Bladon, P. T. "The Human Skin" Edward Arnold Ltd., 1985. pp. 1-3, 6-10, 20-26.
[3] Lanir, Y. "Skin Mechanics" Chapter in: Handbook of Bioengineering, McGraw-Hill, 1987. pp. 11.1-11.25
[4] Brown, I. A. "Scanning electron microscopy of human dermal fibrous tissue." Journal of Anatomy, 1972, 113, pp. 159-68.
[5] Gray, H., Warren H. L. "Anatomy of the Human Body" Bartleby.com, 2000.
[6] Ruegg, J. C. "Calcium in Muscle Activation" Springer-Verlag, 1986. pp. 1-5.
[7] Hunter, P. J."Myocardial constitutive laws for continuum models of the heart" Chapter in: Molecular and subcellular cardiology, Plenum Press, New York, 1995. pp. 303-318
[8] Parke, F. I. ,. Keith W. "Computer Facial Animation" A K Peters, Ltd, 1996. pp. 187-196.
[9] Parke, F.I. "Parameterized models for facial animation" IEEE Computer Graphics and Applications, 1982, 2, pp. 61.
[10] Keeve, E., Girod, S., Kikinis, R. and Girod, B. "Deformable modeling of facial tissue for craniofacial surgery simulation" Computer Aided Surgery, 1998, 3, pp. 228-238.
[11] Koch, R. M. et al. "Simulating facial surgery using finite element models" Proceedings of the 23rd annual conference on Computer graphics and interactive techniques - SIGGRAPH 96, 1996, pp. 421.
[12] Sifakis E., Neverov I., Fedkiw R. "Automatic determination of facial muscle activations from sparse motion capture marker data" ACM Transactions on Graphics, 2005, 24, pp. 417.
[13] Chabanas, M "Patient specific finite element model of the face soft tissues for computer-assisted maxillofacial surgery" Medical Image Analysis, 2003, 7, pp. 131.
[14] Zhang, Y., Sim, T. "Realistic and efficient wrinkle simulation using an anatomy-based face model with adaptive refinement" International 2005 Computer Graphics, 2005, pp. 3.
[15] Li, M., Yin, B, K., D. "Modeling expressive wrinkles of face For animation" Fourth International Conference on Image and Graphics (ICIG 2007), 2007, pp. 874.
[16] Wu, Y., Beylot, P. and Thalmann, N. M. "Skin aging estimation by facial simulation" Proceedings Computer Animation 1999 CA-99, 1999, pp. 210.
[17] Wu, Y., Thalmann, N. and Thalmann, D. "A plastic-visco-elastic model for wrinkles in facial animation and skin aging" Proc. Pacific Conference 94, 1994, pp. 201-213.
[18] Flynn, C. and McCormack, B. A. O. "Finite element modelling of forearm skin wrinkling." Skin research and technology, 2008, 14, pp. 261-9.
[19] Magnenat-Thalmann, N. et al. "A computational skin model: fold and wrinkle formation" IEEE Transactions on Information Technology in Biomedicine, 2002, 6, pp. 317.
[20] Hendriks, F. M. et al. "A numerical-experimental method to characterize the non-linear mechanical behaviour of human skin" Skin Research and Technology, 2003, 9, pp. 274.
[21] Herzog, W. "Skeletal Muscle Mechanics: From Mechanism to Function" John Wiley and Sons, 2000. pp. 209.
[22] CMISS [Online]. Available: http://www.cmiss.org
[23] Ackerman, M.J. "The Visible Human Project" Proceedings of the IEEE, 1998, 86, pp. 504.
[24] Shuster, S., Black, M. and McVitie E. "The influence of age and sex on skin thickness, skin collagen and density" British Journal of Dermatology, 1975, 93, pp. 639.
[25] Lanir, Y. "Constitutive equations for fibrous connective tissues" Journal of Biomechanics, 1983, 16, pp. 1-12.